Measurement of the shear strain of the Gd2O3/GaAs(001) interface by photoreflectance difference spectroscopy

N. A. Ulloa-Castillo, L. F. Lastras-Martínez, R. E. Balderas-Navarro, R. Herrera-Jasso, and A. Lastras-Martínez

Citation: Applied Physics Letters **105**, 181905 (2014); doi: 10.1063/1.4901168
View online: http://dx.doi.org/10.1063/1.4901168
View Table of Contents: http://scitation.aip.org/content/aip/journal/apl/105/18?ver=pdfcov
Published by the AIP Publishing

Measurement of the shear strain of the Gd_2O_3/GaAs(001) interface by photoreflectance difference spectroscopy

N. A. Ulloa-Castillo,[1,a)] L. F. Lastras-Martínez,[1,b)] R. E. Balderas-Navarro,[1,2,c)] R. Herrera-Jasso,[1] and A. Lastras-Martínez[1]
[1]*Instituto de Investigación en Comunicación Óptica, Universidad Autónoma de San Luis Potosí, Alvaro Obregón 64, San Luis Potosí 78000, Mexico*
[2]*Paul-Drude-Institut für Festkörperelektronik, Hausvogteiplatz 5-7, 10117 Berlin, Germany*

(Received 2 August 2014; accepted 27 October 2014; published online 6 November 2014)

In this work, we report on photoreflectance (PR) and photoreflectance-difference (PR-D) measurements of GaAs(001) upon deposition of Gd_2O_3 thin films. The study is focused on two different substrates: a semi-insulating (SI) with Cr impurities and a Si-doped *n*-type. PR-D results show that Gd_2O_3 induces a tensile strain on the GaAs surface and a direct piezo-electric dipole is created. Such strain changes the crystal symmetry from cubic to orthorhombic and renders the quadratic electro-optic (QEO) component anisotropic. For the SI substrate, both linear electro-optic (LEO) and QEO components contribute to the PR-D spectrum, whereas the *n*-type PR-D spectrum is dominated by the LEO component. In both cases, a tensile strain induces a rigid redshift of $\sim$20 meV to low energies of the E_1 and $E_1 + \Delta_1$ optical transitions. © *2014 AIP Publishing LLC*. [http://dx.doi.org/10.1063/1.4901168]

The high-κ dielectric/III-V interface is extremely important for metal-oxide-semiconductor (MOS) technology and can exhibit either a high or low interface state density depending on both the intrinsic properties of III-V surfaces and the nature of their oxidation chemistry.[1,2] In particular, Gd_2O_3 has been investigated due to its high dielectric constant,[3,4] large band gap[5] and excellent thermodynamical stability in semiconductors.[6,7] As a matter of fact, a low interfacial density of states was demonstrated in Gd_2O_3/GaAs MOS devices.[8,9] However, as GaAs has piezo-electric character, a polarization charge will be induced by the stress at the insulator-semiconductor interface when the dielectric layer is deposited, thus modifying the electric properties at the interface by this induced charge. In this regard, probing of interface states evolution for process control during interface formation is of particular importance, preferably *in situ*. Optical spectroscopies are non-invasive and can be operated in any environment.

Two linear optical spectroscopies employed to probe surface piezo-electric phenomena in semiconductors are reflectance-difference (RD) and photoreflectance-difference (PR-D) spectroscopies.[10–13] On the (001) surface of zinc-blende semiconductors, RD measures the difference in reflectivity between [110] and [1$\bar{1}$0] light polarizations,[10,14] whereas PR-D accounts for the difference between a PR spectrum for polarized probe light (along either [110] or [1$\bar{1}$0]) and the corresponding spectrum for unpolarized probe light.[15] Furthermore, PR spectra comprise both linear electro-optic (LEO) and quadratic electro-optic (QEO) components. PR-D spectra involve only the LEO component as the QEO contribution is nominally isotropic. However, when the crystal symmetry is modified, as in the case of an external stress applied along [110], the QEO component becomes anisotropic as well.[16] For instance, the strain caused by dimers at the GaAs(001)-c(4 × 4) surface reconstruction induces a direct piezo-electric dipole (DPD) that opposes the electric field (F) of the space-charge layer within the first tens monolayers into the crystal.[10] Another example is the hydrocarbon ring molecule adsorption onto the As surface dimers of GaAs(001)-c(4 × 4), which reduces the surface band bending causing an increment of F.[17] Therefore, a modification of the surface states influences significantly the surface electro-optical properties.[18]

In this work, we report on *in situ* PR and PR-D measurements of two GaAs(001) surfaces: a semi-insulating (SI) with Cr impurities and a Si-doped *n*-type. PR and PR-D measurements were done around E_1 and $E_1 + \Delta_1$ optical transitions in order to investigate changes of the surface states caused by modifications in the surface electric field upon deposition of Gd_2O_3 on GaAs. The results for the SI substrate show that Gd_2O_3 modifies the GaAs(001) by building up a tensile shear strain which renders the QEO component anisotropic, whereas, for the *n*-type substrate, the LEO component dominates the lineshapes even after Gd_2O_3 deposition. We note that, because we are interested on the PR-D evolution upon surface modifications, the critical points at E_1 (2.92 eV) and $E_1 + \Delta_1$ (3.13 eV) optical transitions were used, as the penetration depth of the probe light is only 170 Å for GaAs. This contrasts the case at E_0 (1.42 eV), where probe light can penetrate down to the back-face in thin GaAs substrates, thus washing out any optical anisotropy coming from the front surface.

PR and PR-D measurements were carried out in ultra-high vacuum (UHV) on the S1 and S2 substrates which are described in Table I. Both samples were chemical etched in H_2O:H_2SO_4:H_2O_2 (1:5:1) and immediately introduced into the UHV chamber. The samples were then heated up gradually to obtain a clear (1 × 1) reconstruction as monitored by

[a)]Electronic mail: nulloa@cactus.iico.uaslp.mx
[b)]Electronic mail: lflm@cactus.iico.uaslp.mx
[c)]Electronic mail: rbn@cactus.iico.uaslp.mx and balderas@pdi-berlin.de

TABLE I. Samples used for the Gd_2O_3 deposition.

Sample	Substrate
S1	SI-GaAs(001):Cr
S2	*n*-GaAs(001) ($n \sim 10^{17}\,cm^{-3}$)

RHEED. The deposition of Gd_2O_3 was performed through an *e*-beam evaporator operated at a high voltage of 1.1 KV with an emission current of 60 mA. The temperatures of samples S1 and S2 were T = 350 °C. The base pressure in the UHV chamber was maintained at $P_{base} = 8 \times 10^{-10}$ Torr, and the maximum pressure registered during the evaporations was $P_{max} = 4 \times 10^{-8}$ Torr. The whole process was monitored with a residual gas analyzer, and the deposition of Gd_2O_3 was probed in real time using the RD spectrometer in order to register changes in the surface anisotropy response as induced by the Gd_2O_3 deposition. Our criterion was to keep going on with the Gd_2O_3 deposition until changes in the RD signal became detectable. The thicknesses of the deposited Gd_2O_3 films were estimated by a scanning electron microscope in *ex situ* mode and were found to be ~20 nm and ~40 nm for samples S1 and S2, respectively.

For the optical measurements, a photoelastic modulator (PEM)-based spectrometer was attached through a strain-free optical viewport into the UHV chamber. For further experimental details concerning the operation of this spectrometer, see Ref. 15.

Fig. 1 shows the energy bands of sample S1 under different surface conditions. Fig. 1(a) represents the energy bands for a clean surface. Fermi level at the surface is pinned at around midgap,[19,20] a weak electric field is formed, and flat bands are expected due to the lack of free carriers. Under this situation, when the laser beam in a PR experiment impinges the sample, electron-hole pairs are both created and spatially separated through a Dember effect due to the difference in diffusion constants for holes and electrons.[21] In this case, a Dember electric field (F_D) is induced causing a band profile as is shown in Fig. 1(b). Fig. 1(c) shows the band diagrams of GaAs after the deposition of a Gd_2O_3 layer. Gd_2O_3 is an ionic crystal with a lattice constant of 10.81 Å.[5,22] In contrast, the bonds in GaAs are mostly covalent and the crystal has a lattice constant of 5.65 Å. In consequence, due to the difference in lattice constants between Gd_2O_3 and GaAs, a surface tensile stress induces a strain field that penetrates into the GaAs crystal. This strain produces a DPD and the piezo-electric field (F_{DPD}) associated to the DPD contributes to the band profile as shown in Fig. 1(c). When the laser beam reaches this surface, the electon-hole pairs partially screen the piezo-electric field by an amount F, thus reducing the band bending as is illustrated in Fig. 1(d). Note that, additional to the Dember effect, the PR spectrum includes the component associated to the screening (i.e., by F) of the $F_{DPD,}$ which is expected to be larger than the Dember modulation and therefore dominates the PR mechanism.[23] By comparing the band profiles of Figs. 1(a)–1(d), the PR lineshape of Gd_2O_3/S1 sample is expected to have an opposite sign in comparison to that of clean-S1.

The PR spectra of the clean-S1 and Gd_2O_3/S1 are shown in Fig. 2. Two differences can be pointed out: the strength of the PR spectra of the clean-S1 sample is approximately 2 times larger than the spectra of Gd_2O_3/S1; additionally, PR spectra are reversed in sign and exhibit different lineshapes, confirming the band model discussed above.

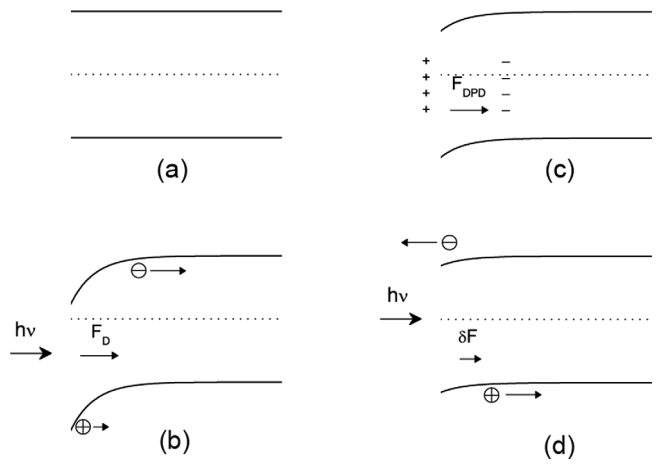

FIG. 1. Band diagrams schematics for a semi-insulating GaAs crystal under different surface conditions. Clean surface in the dark (a) and under laser irradiation (b). In case (a), flat bands condition is obtained, while in case (b), a charge dipole F_D is induced due to the difference in diffusion constants for holes and electrons due to the Dember effect. (c) GaAs surface after the deposition of a Gd_2O_3 layer. This layer induces a piezo-electric field (F_{DPD}) that bends the bands. The band bending in case (c) can be reduced upon laser irradiation as is shown in (d) by a screening of the F_{DPD} field by $\delta F = F_{DPD} - F$. F is the field induced by photoelectrons when the laser impinges the sample.

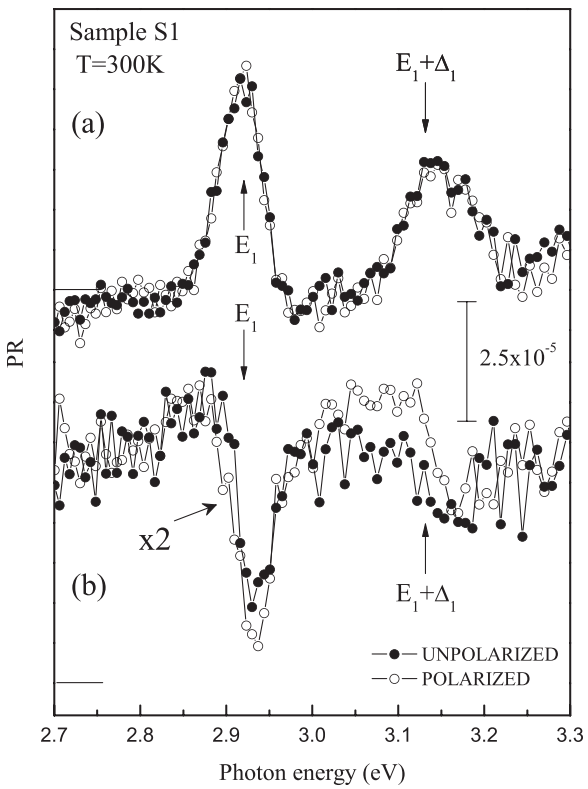

FIG. 2. Photoreflectance spectra for sample S1 (a) before deposition and (b) after deposition of Gd_2O_3. The spectra represented by open and solid symbols were taken with polarized probe light along [110] and with unpolarized probe light, respectively.

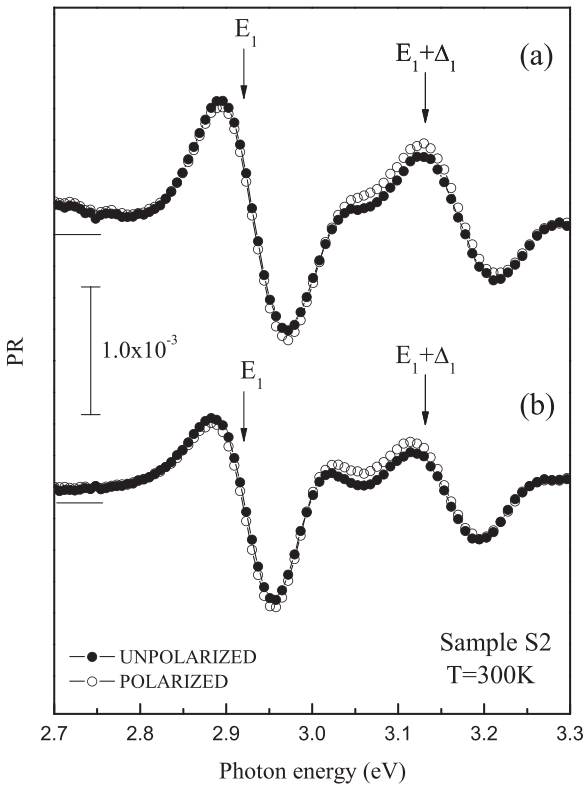

FIG. 3. Photoreflectance spectra for sample S2 (a) before deposition and (b) after deposition of Gd_2O_3. The spectra represented by open and solid symbols were taken with polarized probe light along [110] and with unpolarized probe light, respectively.

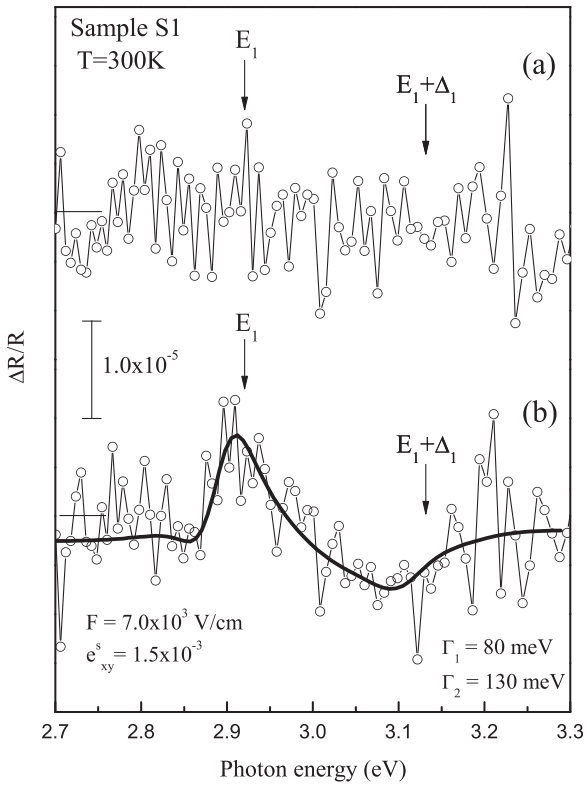

FIG. 4. Photoreflectance-difference spectra of sample S1 (a) before deposition and (b) after deposition of Gd_2O_3. After deposition of Gd_2O_3, a strain is induced on the GaAs surface and a piezo-electric field is created. The solid line represents the fit obtained with Eq. (1) considering the fitting parameters indicated in the figure, where $\Gamma_1(\Gamma_2)$ is the broadering parameter for $E_1(E_1+\Delta_1)$ optical transition.

For sample S2, a surface electric field is generated due to the Si doping and consequently a band bending. Fig. 3 shows PR spectra of the clean-S2 and Gd_2O_3/S2 samples. It can be seen that their lineshapes are less sensible than in the case of the sample S1 and also that the strengths of the PR signals are at least one order of magnitude larger than for the case of sample S1.

Fig. 4 shows the PR-D spectra for sample S1 retrieved from the data in Fig. 2. As we can see in Fig. 4(a), before deposition of Gd_2O_3, the surface electric field is close to zero as we expect from the band diagram of SI-GaAs in Fig. 1(a). In addition, the Dember effect responsible for the PR signal appears too weak to produce a measurable signal; such value has been estimated to be in the range of $\sim$260 V/cm.[24] After deposition of Gd_2O_3, as shown in Fig. 4(b), a strain is induced on the GaAs surface and a DPD has built up.

For sample S2, Fig. 5 shows the corresponding PR-D results from the PR spectra in Fig. 3. As it was expected, the lineshapes before and after deposition of Gd_2O_3 are similar, which is an indicative that the surface electric field induced by the native carrier concentration is larger than the F_{DPD}. Furthermore, as discussed below, the deposition of the Gd_2O_3 layer decreases the strength of the surface electric field.[9]

In order to model the interfacial electric field formed between Gd_2O_3 and the corresponding substrate, we have used the PR-D lineshape in the region of the E_1 and $E_1+\Delta_1$ optical transitions, given by[10]

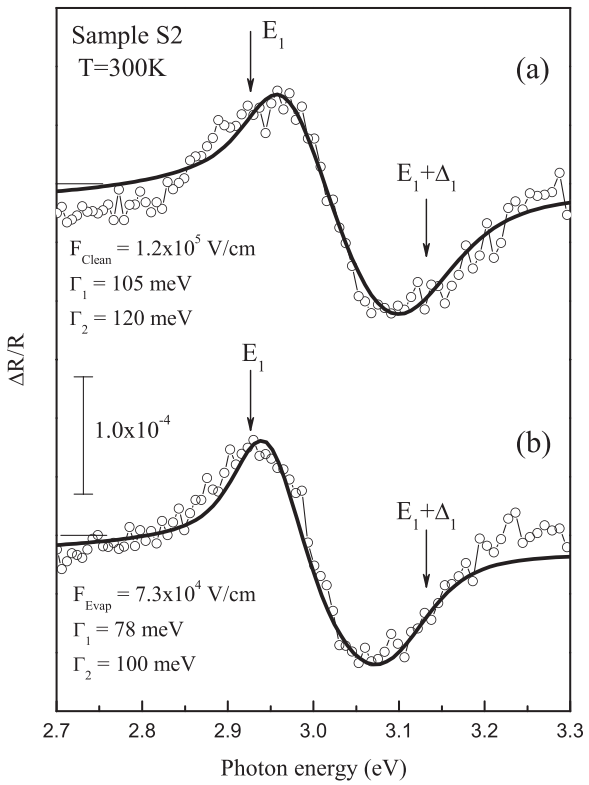

FIG. 5. Photoreflectance-difference spectra of sample S2 (a) before deposition and (b) after deposition of Gd_2O_3. The solid lines represent the fits obtained with Eq. (1) considering the fitting parameters indicated in the figure, where $\Gamma_1(\Gamma_2)$ is the broadering parameter for $E_1(E_1+\Delta_1)$ optical transition.

$$\frac{\Delta R}{R} = Re\left[(\alpha - i\beta)\left(r\frac{4D_3^5}{\sqrt{6}\Delta_1}\epsilon(E, E_1 + \Delta E_{so} + \Delta E_h)d_{14}\mathrm{F} + \frac{D_1^5}{2\sqrt{3}E^2}\frac{\partial E^2\epsilon(E, E_1 + \Delta E_{so} + \Delta E_h)}{\partial E}d_{14}\mathrm{F}\right)\right] + r\frac{4D_3^5}{\sqrt{6}\Delta_1}L(E, E_1 + \Delta E_{so} + \Delta E_h)e_{xy}^s + \frac{D_1^5}{2\sqrt{3}}\frac{\partial L(E, E_1 + \Delta E_{so} + \Delta E_h)}{\partial E}e_{xy}^s, \quad (1)$$

where, α and β are the Seraphin coefficients, e_{xy}^s the surface strain, d_{14} the converse piezo-electric coefficient ($d_{14} = -2.7 \times 10^{-10}$ cm/V), D_1^5 the interband orthorhombic deformation potential for transitions of symmetry Λ ($D_1^5 = 8.8$ eV), D_3^5 an orthorhombic deformation potential for the valence band ($D_3^5 = -7.6$ eV), Δ_1 the spin orbit splitting energy for the valence band ($\Delta_1 = 0.22$ eV), $r = +1(-1)$ refers to E_1 ($E_1 + \Delta_1$), and F is the field induced by photoelectrons when the laser impinges the sample (see Fig. 1(d)); ϵ is the dielectric function of the sample, L is the quadratic component of the PR, and ΔE_{so} and ΔE_h are defined in Ref. 16. The first two terms of Eq. (1) correspond to the LEO component and the last two correspond to the QEO component.[10]

The results of the fitting procedure outlined by Eq. (1) are shown in Figs. 4(b) and 5 for samples S1 and S2, respectively. For sample S1, we found that both LEO and QEO components contribute significantly to the PR-D spectrum. The best fit was obtained by using the values of e_{xy}^s and F listed in Table II. The electric field associated to the DPD has a value of $F_{DPD} = e_{xy}^s(\sqrt{3}e_{14})/(\epsilon_0\epsilon_r)$ along the [001] direction, where ϵ_0 is the permittivity of vacuum, ϵ_r the static dielectric constant, $e_{14} = d_{14}/S_{44}$ is the direct piezo-electric coefficient, and S_{44} is the stiffness component. One can further estimate the interfacial state density (D_{it}) involved in the interface formation by assuming that the D_{it} is directly linked to the F_{DPD}. This value is given by $D_{it} = \sqrt{3}e_{14}e_{xy}^s/q$, where q is the free electron charge. By taking the values of $e_{14} = -0.16\,\mathrm{C/m^2}$, $\epsilon_r = 12.5$, and $\epsilon_0 = 8.854 \times 10^{-12}$ F/m, one obtains $D_{it} = 2.6 \times 10^{11}\,\mathrm{cm^{-2}eV^{-1}}$, which compares well with the D_{it} found for $Ga_2O_3(Gd_2O_3)$/GaAs, measured previously using the *C-V* quasistatic/high frequency method, in the range from 2×10^{10} to $5 \times 10^{12}\,\mathrm{cm^{-2}eV^{-1}}$ at various band gap energies.[25,26]

To achieve a satisfactory fit for sample S2, only the LEO component was sufficient, indicating that the electric field F_{Clean} associated to the doping level is larger than the corresponding F_{DPD}, and consequently the QEO component accounting for the shear strain is negligible. Indeed, the surface electric field of sample S2 decreases upon deposition, and is due to the passivation character of the Gd_2O_3 film (see Table II). The decrease in the broadering parameters for the E_1 and $E_1 + \Delta_1$ transitions attests the modification of the surface electric field in this sample. Finally, for both samples, the presence of the tensile surface strain induces a hydrostatic redshift ΔE_h of the E_1 and $E_1 + \Delta_1$ transitions: the fits in Figs. 4(b) and 5(b) were rigidly shifted to lower energies by $\Delta E_h = 23$ meV and $\Delta E_h = 21$ meV, respectively. Note the excellent agreement between the experiments and the PR-D piezo-electric strain model described by Eq. (1).

TABLE II. Surface shear strain and electric field strengths.

Sample description	e_{xy}^s	[V/cm]
Gd_2O_3/S1	1.5×10^{-3}	$F = 7 \times 10^3$
Clean-S2	…	$F_{Clean} = 1.2 \times 10^5$
Gd_2O_3/S2	…	$F_{Evap} = 7.3 \times 10^4$

In conclusion, Gd_2O_3 thin films were deposited on SI-GaAs(100):Cr and *n*-type GaAs(001) commercial substrates. Polarization contrast optical probes were employed to investigate the possibility that the Gd_2O_3 film exerts a strain field in a region close to the Gd_2O_3/GaAs interface. Specifically, PR-D measurements of SI-GaAs clearly indicate that a shear strain e_{xy}^s within the range of 10^{-3} is built up and a piezo-electric field associated to the DPD is created in the Gd_2O_3/GaAs interface. Such DPD is proposed to be correlated to the appearance of interface states. The results obtained for *n*-type GaAs show that the native surface electric field, which is larger than the DPD, dominates the lineshape even after the deposition of Gd_2O_3. However, it was shown that the PR-D spectroscopy is able to detect changes in this native surface electric field upon passivation.

The results reported in this paper show that the optical probe employed is suitable to shed light onto details of the interface formed between high-κ dielectric materials and (001)-oriented zincblende semiconductors on a quantitative basis; in particular, on the existence of interfacial strain and evolution of native electric fields during effective passivation, which are important processes in MOS-based technology.[1,27]

This work was supported by Consejo Nacional de Ciencia y Tecnología (Mexico, Grant Nos. 79635/207216, 130009, and 81316) and FAI-UASLP. The autors would like to thank E. Ontiveros-Hernández, F. J. Ramírez-Jacobo, and J. González-Fortuna for their technical expertise.

[1]See, for example, J. A. del Alamo, Nature **479**, 317 (2011); Z. Jiang, C. Yuan, and S. Ye, RSC Adv. **4**, 19584 (2014).
[2]M. Caymax, G. Brammertz, A. Delabie, S. Sioncke, D. Lin, M. Scarrozza, G. Pourtois, W.-E. Wanga, M. Meuris, and M. Heyns, Microelectron. Eng. **86**, 1529 (2009).
[3]G. D. Wilk, R. M. Wallace, and J. M. Anthony, J. Appl. Phys. **89**, 5243 (2001).
[4]K. Xu, R. Ranjith, A. Laha, H. Parala, A. P. Milanov, R. A. Fischer, E. Bugiel, J. Feydt, S. Irsen, T. Toader, C. Bock, D. Rogalla, H.-J. Osten, U. Kunze, and A. Devi, Chem. Mater. **24**, 651 (2012).
[5]C. Steiner, B. Bolliger, M. Erbudak, M. Hong, A. R. Kortan, J. Kwo, and J. P. Mannaerts, Phys. Rev. B **62**, R10614 (2000).
[6]M. Gasgnier, J. Mater. Sci. **26**, 1989 (1991).
[7]L. S. Wang, J. P. Xu, L. Liu, W. M. Tang, and P. T. Lai, Appl. Phys. Express. **7**, 061201 (2014).
[8]Y. L. Huang, P. Chang, Z. K. Yang, Y. J. Lee, H. Y. Lee, H. J. Liu, J. Kwo, J. P. Mannaerts, and M. Hong, Appl. Phys. Lett. **86**, 191905 (2005).
[9]J. S. Hwang, Y. C. Wang, W. Y. Chou, S. L. Tyan, M. Hong, J. P. Mannaerts, and J. Kwo, J. Appl. Phys. **83**, 2857 (1998).
[10]L. F. Lastras-Martínez, J. M. Flores-Camacho, A. Lastras-Martínez, R. E. Balderas-Navarro, and M. Cardona, Phys. Rev. Lett. **96**, 047402 (2006).
[11]A. Ohtake, J. Nakamura, S. Tsukamoto, N. Koguchi, and A. Natori, Phys. Rev. Lett. **89**, 206102 (2002).
[12]L. F. Lastras-Martínez, R. E. Balderas-Navarro, A. Lastras- Martínez, and K. Hingerl, Semicond. Sci. Technol. **19**, R35 (2004).

[13]A. Lastras-Martínez, R. E. Balderas-Navarro, P. Cantú-Alejandro, and L. F. Lastras-Martínez, J. Appl. Phys. **86**, 2062 (1999).
[14]D. E. Aspnes and A. A. Studna, Phys. Rev. Lett. **54**, 1956 (1985).
[15]A. Lastras-Martínez, R. E. Balderas-Navarro, L. F. Lastras-Martínez, and M. A. Vidal, Phys. Rev. B **59**, 10234 (1999).
[16]L. F. Lastras-Martínez, M. Chavira-Rodríguez, A. Lastras-Martínez, and R. E. Balderas-Navarro, Phys. Rev. B **66**, 075315 (2002).
[17]T. Bruhn, B.-O. Fimland, M. Kneissl, N. Esser, and P. Vogt, Phys. Rev. B **83**, 045307 (2011).
[18]G. M. Marshall, G. P. Lopinski, F. Bensebaa, and J. J. Dubowski, Nanotechnology **22**, 235704 (2011).
[19]J. V. DiLorenzo and D. D. Khandelwal, *GaAs FET Principles and Technology* (Artech House, 1982).
[20]Y. F. Hu, C. C. Ling, C. D. Beling, and S. Fung, J. Appl. Phys. **82**, 3891 (1997).
[21]M. B. Johnston, D. M. Whittaker, A. Corchia, A. G. Davies, and E. H. Lineld, Phys. Rev. B **65**, 165301 (2002).
[22]E. J. Nelson, J. C. Woicik, M. Hong, J. Kwo, and J. P. Mannaerts, Appl. Phys. Lett. **76**, 2526 (2000).
[23]D. E. Aspnes, Phys. Rev. Lett. **28**, 168 (1972).
[24]R. Wang and D. Jiang, J. Appl. Phys. **72**, 3826 (1992).
[25]M. Hong, M. Passlack, J. P. Mannaerts, J. Kwo, S. N. G. Chu, N. Moriya, S. Y. Hou, and V. J. Fratello, J. Vac. Sci. Technol. **14**, 2297 (1996).
[26]M. Passlack, M. Hong, J. P. Mannaerts, R. L. Opila, S. N. G. Chu, N. Moriya, F. Ren, and J. Kwo, IEEE Trans. Electron Devices **44**, 214 (1997).
[27]M. Hong, A. R. Kortan, J. Kwo, J. P. Mannaerts, J. J. Krajewski, Z. H. Lu, K. C. Hsieh, and K. Y. Cheng, J. Vac. Sci. Technol. B **18**, 1453 (2000).